

# 小型掠入射式近边 X 射线吸收谱仪的设计

陈晨曦<sup>1,2</sup>, 金春水<sup>1\*</sup>, 王君<sup>1</sup>, 谢耀<sup>1</sup>

(1. 中国科学院 长春光学精密机械与物理研究所 应用光学国家重点实验室, 吉林 长春 130033;  
2. 中国科学院大学, 北京 100049)

**摘要:** 近边 X 射线吸收精细结构(NEXAFS)谱包含了吸收原子的局域结构信息,由于其适用范围广,灵敏度高,已经成为研究物质结构的重要手段之一。为了研究有机物的碳 1s NEXAFS 谱,本文基于气体激光等离子体 X 射线光源,采用具有平场特性的凹面变线距光栅作为分光元件,面阵 CCD 作为光谱探测器,设计了一台小型掠入射式近边 X 射线吸收谱仪。通过优化光栅和 CCD 的装配方案,得到了入射角 88.6°的装配参数。利用光线追迹法分析了谱仪的分辨率,该谱仪工作波段 2~5 nm,在 4.4 nm 处分辨率可达 666。通过分析各结构参量误差对谱线半高宽的影响发现,半高宽对入射角的误差最为敏感,优化的装配方案可以实现入射角的高精度调节。利用氮气等离子体光谱测试了光谱仪的性能,结果显示分辨率达到设计指标。

**关键词:** 光谱仪;近边 X 射线吸收;掠入射;优化的装配方案;分辨率

中图分类号: O434.13 文献标识码: A doi: 10.3788/CO.20181102.0265

## Design of a compact spectrometer under grazing incidence conditions for near-edge X-ray absorption spectroscopy

CHEN Chen-xi-yang<sup>1,2</sup>, JIN Chun-shui<sup>1\*</sup>, WANG Jun<sup>1</sup>, XIE Yao<sup>1</sup>

(1. *Changchun Institute of Optics, Fine Mechanics and Physics, Chinese Academy of Sciences, Changchun 130033, China;*  
2. *University of Chinese Academy of Sciences, Beijing 100049, China*)

\* *Corresponding author, E-mail: Jincs@sklao.ac.cn*

**Abstract:** Near edge X-ray absorption fine structure(NEXAFS) spectrum contains the local structure information of the absorbing atoms. Due to its wide range of applications and high sensitivity, it has become an important method to study the structure of materials. In order to study the NEXAFS spectrum of carbon in organic substances, a design of a compact spectrometer under grazing incidence conditions is presented, based on a laser-produced plasma source using a gas target. An aberration corrected flat-field grating and a CCD camera are used to detect the spectrum. To achieve the high precision adjustment of the incident angle of the grating, an optimized scheme where the incident angle is 88.6° has been given. Using ray tracing, the resolution of the

收稿日期: 2017-10-15; 修订日期: 2017-11-28

spectrometer is analyzed. It is about 666 at 4.4 nm in the wavelength range of 2–5 nm. From the influence of each parameter error on the image width, it is found that the error of the incident angle is the most sensitive, and using the optimized assembly scheme is able to achieve the high accuracy adjustment of the incident angle. The performance of the spectrometer has been tested using the nitrogen plasma spectrum, and the results show that the resolution reaches the design index.

**Key words:** spectrometer; near edge X-ray absorption; grazing incidence; optimized assembly scheme; resolution

## 1 引言

### Introduction

近边 X 射线吸收精细结构(Near Edge X-ray Absorption Fine Structure, NEXAFS) 光谱是由吸收原子的内层电子吸收光子跃迁到外层的空轨道产生的<sup>[1]</sup>, 反映了吸收原子与周围原子间的相互作用, 因此通过分析近边结构可以获得吸收原子的电子结构和近邻几何结构信息。与电子能量损失谱(EELS) 和 X 射线拉曼散射(XRS) 等方法相比<sup>[2]</sup>, NEXAFS 技术不易造成辐射损伤, 对样品的物理状态没有要求, 适用范围广泛。起初, 这项技术仅仅用于研究小分子, 随着理论和实验技术的发展, 如今, 它已经广泛应用于各种复杂大分子的研究, 例如有机高分子材料<sup>[3-4]</sup>, 土壤、大气中的天然有机物<sup>[5-6]</sup>, 甚至是水环境中的生物分子<sup>[7]</sup>。

Near Edge X-ray Absorption Fine Structure (NEXAFS) spectrum is produced due to transition of the inner electrons of absorbing atoms to the outer unoccupied molecular orbital by absorbing photons<sup>[1]</sup> and reflects the interaction of absorbing atoms with ambient atoms, so the information on the electron structure and adjacent geometric structure of absorbing atoms can be obtained through analyzing the near edge structure. In comparison with the methods such as electron energy loss spectroscopy(EELS), X-ray Raman Scattering(XRS), etc.<sup>[2]</sup>, the NEXAFS technology doesn't result in radiation damage easily and has no requirements for the physical state of samples, so it has a wide range of application. At first, this technology was only used to study small

molecules. With the development of theories and experimental technologies, it has now been extensively applied in the study of various complex macromolecules, e. g. organic polymer materials<sup>[3-4]</sup>, natural organic substances in soils and atmosphere<sup>[5-6]</sup>, and even biomolecules in water environment<sup>[7]</sup>.

目前, 国内外大多数 NEXAFS 实验都是在同步辐射线上进行的, 然而同步辐射装置机时非常有限, 且建造运营成本极高, 短期内难以满足大量 NEXAFS 科研需求。因此, 研究基于小型 X 射线光源的实验装置具有重要研究意义和实用价值。近年来, 国内外的研究人员已经基于激光等离子体光源开展了许多相关工作。Osamu Yoda 等人<sup>[8]</sup>利用超环面镜收集 X 射线、平场光栅和弯晶分别对低能和高能光子分光, 微通道检波器二极管阵列系统作为探测器, 设计了一套工作在 100 ~ 3 000 eV 的吸收谱仪; Hidetoshi Nakano 等人<sup>[9]</sup>使用了两个凹面镜将 X 射线聚焦到样品上, 用平场光栅分光, 再由微通道检波器和 CCD 接收, 在 12 nm 处分辨率( $\lambda/\Delta\lambda$ ) 250; U Vogt 等人<sup>[10]</sup>利用透射光栅和 CCD 搭建了一台用于水窗波段的实验装置, 成功获得了  $\beta$  胡萝卜素的近边吸收谱, 但是这套装置在 4.4 nm 处的分辨率只有 300, 不足以区分有机物吸收谱的所有典型峰, 后来他们用离轴反射波带片取代了透射光栅<sup>[11]</sup>, 分辨率提高了一倍, 获得的聚酰亚胺和 PET (poly ethylene terephthalate) 薄膜的近边吸收谱均与同步辐射上的实验结果相当; Christian Peth 等人<sup>[12]</sup>研制的吸收谱仪以消像差的平场光栅作为分光器, 背照射式 CCD 作为探测器, 在 2.87 nm 处分辨率 200, 他们使用这套设备研究了高分子材料、生物样品以及土壤提取物的 NEXAFS 谱<sup>[12, 7, 13]</sup>。

At present, most domestic and foreign NEXAFS experiments are conducted on synchrotron radiation lines, but the machine-hour of synchrotron radiation facilities is very limited. Their construction and operation cost is extremely high, and they are difficult to meet the needs of plentiful NEXAFS scientific studies in short term. Hence, the research on the experimental equipment based small X-ray sources has vital research significance and practical value. In recent years, domestic and foreign researchers have carried out a lot of relevant work based on a laser plasma source. Osamu Yoda *et al.*<sup>[8]</sup> designed a set of absorption spectroscopy apparatus working at 100–3 000 eV using toroidal mirrors to collect X-rays, using flat-field gratings and bent crystals to carry out light splitting of low energy and high energy photons respectively and using a micro-channel detector diode array system as a detector. Hidetoshi Nakano *et al.*<sup>[9]</sup> used two concave mirrors to focus X-rays onto samples, flat-field gratings to carry out light splitting, and used micro-channel detectors and CCD to receive information, with the resolution at 12 nm being  $(\lambda/\Delta\lambda)$  250. U Vogt *et al.*<sup>[10]</sup> erected a set of experimental equipment in the water window using transmission gratings and CCD; with the equipment, they successfully obtained the near edge absorption spectrum of  $\beta$  carotene, but the resolution of the equipment was only 300 at 4.4 nm and it was not enough to differentiate all typical peaks of the absorption spectrum of organic substances. Afterwards, they replaced transmission gratings with off-axis reflection zone plates<sup>[11]</sup>, the resolution of the equipment was increased by 100%, and the obtained near edge absorption spectrum of both polyimide and poly ethylene terephthalate (PET) film was equivalent with the experimental result from synchrotron radiation. Christian Peth *et al.*<sup>[12]</sup> developed an absorption spectrometer using an aberration-reduced flat-field grating as the light splitter and back-illuminated CCD as the detector. The resolution of the

spectrometer is 200 at 2.87 nm; they studied the NEXAFS spectrum<sup>[12,7,13]</sup> of high polymer materials, biological samples and soil extracts using the spectrometer.

现有的小型 NEXAFS 光谱仪的研究主要采用透射式光路,这种结构只能得到体相信息,为了获得高信噪比的谱线,被测样品一般为无支撑的薄膜结构,且厚度需严格控制,通常为 100 ~ 200 nm,制备困难。而另一种掠入射式光路则对样品厚度没有要求,因为只有表面很薄的分子层产生吸收,反射光较强,信噪比高,能适应较弱光源;同时还具有很强的表面敏感性,可以用于表面分子变化的研究。近年来,具有特殊光电性质的有机材料<sup>[14-16]</sup>的研究越来越多,本文基于掠入射光路,利用小型的气体激光等离子体 X 射线光源,设计了一台用于研究有机材料碳 1s NEXAFS 谱的近边 X 射线吸收谱仪,并对谱仪的分辨率等指标以及元件的装配公差进行了分析。

A transmissive light path is mainly used in the study of the existing compact NEXAFS spectrometers, but with this structure, only bulk phase information can be obtained. In order to obtain high SNR spectral lines, the tested sample is generally an unsupported membrane structure, and its thickness needs to be strictly controlled and tends to be 100–200 nm, so its preparation is difficult. Another grazing incidence light path has no requirement for sample thickness. This is because only the very thin surface molecular layer has an absorption. The reflected lights is strong with high SNR, and the grazing incidence light path is suitable for weak light sources. In addition, it also has a very strong surface sensitivity and can be used in the study of surface molecule variation. In recent years, there are more and more studies of organic materials<sup>[14-16]</sup> with special photoelectric properties. A design of a compact near edge X-ray absorption spectrometer under grazing incidence conditions to study the NEXAFS spectrum of organic material carbon(1s) is presented, based on a grazing incidence light path, using a small laser-

produced plasma source. In addition, the resolution of the spectrometer and the fitting allowance of components have been analyzed.

## 2 X 射线吸收谱仪设计

### Design of the X-ray absorption spectrometer

碳的近边吸收精细结构在 280 ~ 320 eV 的能量范围内, 对应波长范围为 3.8 ~ 4.4 nm, 为了研究碳的谱线, 要求谱仪在 3 ~ 5 nm 波段工作。碳的内层电子从 1s 轨道跃迁到外层的未占分子轨道引起的吸收峰的典型能量宽度为 0.5 eV<sup>[11]</sup>, 为了能准确反映碳的 1s NEXAFS 谱的特征, 谱仪在 4.4 nm 处的分辨率须在 600 以上。本文据此要求展开设计。

The corresponding wavelength range of the near edge absorption fine structure of carbon is 3.8 - 4.4 nm within the energy range of 280 - 320 eV. In order to study the spectrum of carbon, the spectrometer is required to work at 3 - 5 nm. The typical energy width of the absorption peak caused by the transition of the inner electrons of carbon from 1s orbital to the outer unoccupied molecular orbital is 0.5 eV<sup>[11]</sup>. In order to accurately reflect the features of the NEXAFS spectrum of carbon(1s), the resolution of the spectrometer shall be over 600 at 4.4 nm. In this paper, the spectrometer has been designed based on above requirements.

#### 2.1 谱仪结构设计

##### Spectrometer structure design

本文采用摄谱法设计近边 X 射线吸收谱仪, 光源产生的“白光”先经过样品再分光, 然后利用一维或二维探测器测定通过样品前后的所有波长光的强度, 从而获得吸收谱, 它能同时获得所有波长光的强度, 无需扫描, 还可以做瞬态光谱分析。

The near edge X-ray absorption spectrometer has been designed using the spectrography in this paper. The “white lights” generated by the light source pass through the sample and then are split. Later on, the intensity of lights with all wavelengths

before and after passing through the sample is measured with a 1D or 2D detector so as to obtain the absorption spectrum. With the spectrometer, the intensity of lights with all wavelengths can be obtained simultaneously without scanning, and a transient spectrum analysis can also be made.

设计的掠入射式近边 X 射线吸收谱仪结构示意图如图 1 所示, 系统由气体激光等离子体光源、样品、狭缝、光栅和 CCD 组成。光源以氪气作为靶材, 经过滤光产生波长 2 ~ 6 nm 的连续谱软 X 射线, 掠入射到样品表面, 反射光经光栅分光, 再由 CCD 测定各波长射线的强度, 结合光源的谱线即可得到包含了吸收信息的反射谱。

The sketch of the structure of the designed near edge X-ray absorption spectrometer under grazing incidence conditions is shown in Fig. 1. The system consists of gas laser plasma source, sample, slit, grating and CCD (camera). Krypton is used as the target light source. 2 - 6 nm continuous spectral soft X-rays are generated through filtering and they are of grazing incidence to the sample surface. The reflected lights are split by the grating, and then the intensity of rays with various wavelengths is measured using the CCD (camera). The reflectance spectrum containing absorption information can be obtained according to the spectral line of the light source.

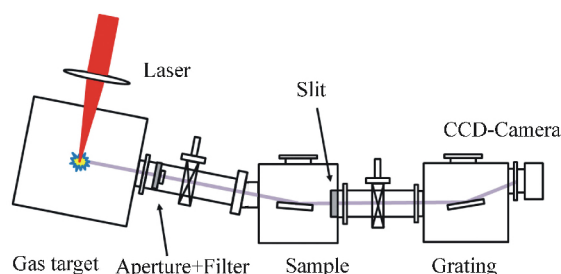


图 1 掠入射式 X 射线吸收谱仪示意图

Fig. 1 Sketch of the designed X-ray absorption spectrometer under grazing incidence conditions

菲涅耳公式给出了反射率与折射率间的关系, 由于存在吸收, 物质对 X 射线的折射率不再是实数, 而是与吸收有关的复数形式  $n = 1 - \delta - i\beta$ , 其中  $1 - \delta$  表示色散,  $\beta$  表示吸收, 由  $\beta$  可以直

接得到线吸收系数  $\mu = 4\pi\beta/\lambda$ , 因此反射率同样包含吸收信息。将复折射率代入菲涅耳公式, 可分别得到掠入射时 p 偏振和 s 偏振的 X 射线反射率, 图 2 为  $\delta = 0.001$  时不同吸收下反射率随入射角的变化曲线, 比较不同偏振光的反射率可知, 无论吸收强弱, 两种偏振光反射率近似相等, 因此, 总反射率可以用 s 偏振光的反射率近似表示:

Fresnel formula gives the relationship between reflectivity and refractive index. Due to existence of absorption, the refractive index of substances to X-ray is not a real number but a complex number related to absorption, *i. e.*  $n = 1 - \delta - i\beta$ , where  $1 - \delta$  denotes dispersion and  $\beta$  denotes absorption. The linear absorption coefficient can be directly obtained from  $\beta$ , *i. e.*  $\mu = 4\pi\beta/\lambda$ . Therefore, reflectivity also contains absorption information. Substitute complex refractive index into Fresnel formula to obtain p-polarized X-ray reflectivity and s-polarized X-ray reflectivity under grazing incidence conditions respectively. Fig. 2 is the curve of variation of reflectivity with incidence angle at different absorption intensity in case of  $\delta = 0.001$ . According to the comparison of reflectivity of different polarized lights, in spite of absorption intensity, the reflectivity of two polarized lights is approximately equal, so the total reflectivity can be expressed approximately in the reflectivity of s-polarized light.

$$R \approx R_s = \left| \frac{\sin(\varphi) - \sqrt{n^2 - \cos^2(\varphi)}}{\sin(\varphi) + \sqrt{n^2 - \cos^2(\varphi)}} \right|^2 \approx \frac{| \varphi - \sqrt{(\varphi^2 - 2\delta) - 2i\beta} |^2}{| \varphi + \sqrt{(\varphi^2 - 2\delta) - 2i\beta} |^2}, \quad (1)$$

式中  $\varphi$  是掠入射角, 可以看出, 反射率  $R(E)$  是  $\delta(E)$  和  $\beta(E)$  的函数,  $E$  为光子能量, 利用公式 (1) 结合数据库 CXRO<sup>[17]</sup> 中得到的  $\delta(E)$  可以从测得的反射率谱线中提取出 NEXAFS 谱。

Where  $\varphi$  is grazing incidence angle. It can be seen that reflectivity  $R(E)$  is the function of  $\delta(E)$  and  $\beta(E)$ , where  $E$  is photon energy. NEXAFS spectrum can be extracted from the measured reflectivity spectral line using formula (1) in combination with  $\delta$

( $E$ ) obtained from the database CXRO<sup>[17]</sup>.

从图 2 可以看出, 反射率总是随掠入射角的增大而减小, 当掠入射角增大到临界角  $\varphi_c$ , 低吸收的反射率迅速下降, 这个角即为全反射临界角。为了使反射率谱线能清晰反映吸收的变化, 谱仪的掠入射角需小于样品的全反射临界角, 考虑到有机物在碳的吸收边 4.4 nm 附近的全反射临界角约为  $3^\circ$ , 因此本文设计的谱仪取  $2^\circ$  掠入射。

As shown in Fig. 2, reflectivity always decreases as grazing incidence angle increases. When grazing incidence angle increases to the critical angle  $\varphi_c$ , the reflectivity at low absorption intensity decreases rapidly. This angle is a critical angle of total reflection. In order that the reflectivity spectral line can clearly reflect absorption variation, the grazing incidence angle of the spectrometer would be less than the sample's critical angle of total reflection. In view of the fact that the critical angle of total reflection of organic substances is about  $3^\circ$  near the carbon's absorption edge of 4.4 nm, the grazing incidence angle of the spectrometer designed in this paper is taken as  $2^\circ$ .

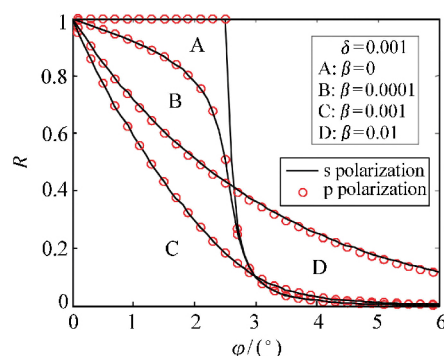


图 2 反射率随掠入射角的变化

Fig. 2 Reflectivity as a function of grazing incidence angle

## 2.2 光栅选型

### Grating selection

分光元件对谱仪的性能具有决定性作用。普通的平面光栅分辨能力较差, 无法满足 X 射线波段的高分辨率要求, 如果增加聚焦镜, 会降低系统的光能利用率。常规的凹面等间距光栅具有分光

和聚焦作用, 但为使像差最小必须采用罗兰圆结构, 不能用平面探测器采集。因此, 本文使用矫正像差的全息变栅距凹球面光栅, 既能同时实现分光 and 聚焦, 又具有平场特性, 便于使用面阵型 CCD 接收。变栅距凹面光栅的原理示意图如图 3 所示, 其中  $x$  轴为光栅中心法线方向,  $y$  轴为光栅中心切线方向,  $\alpha$  为入射角,  $\beta$  为衍射角,  $r$  为入射臂长,  $r'$  为出射臂长。

The light splitting element plays a decisive role in the performance of the spectrometer. The resolution capability of an ordinary plane grating is poor and cannot meet the high resolution requirements of X-ray wavelengths. In case of adding focusing mirrors, the system's efficiency of light energy utilization will be reduced. The conventional concave evenly-spaced grating has functions such as light splitting and focusing, but to minimize aberration, Rowland circle structure must be adopted, and a plane detector cannot be used in acquisition. Therefore, the aberration-corrected holographic varied line-space concave spherical grating is used in this paper, which can achieve both light splitting and focusing and also has flat field characteristics, for convenience of using the area array type CCD to receive

information. The schematic diagram of the aberration corrected flat-field grating is shown in Fig. 3, where  $x$  axis is the central normal direction of the grating,  $y$  axis is the central tangent direction of the grating,  $\alpha$  is incidence angle,  $\beta$  is diffraction angle,  $r$  is incidence arm length, and  $r'$  is emergence arm length.

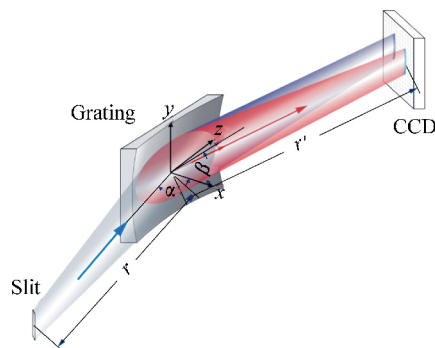


图 3 变栅距凹面光栅原理图

Fig. 3 Schematic diagram of the aberration corrected flat-field grating

利用费马原理<sup>[18]</sup>可以得到光栅色散方程和色散方向的聚焦方程分别为:

Based on Fermat principle<sup>[18]</sup>, the obtained grating's dispersion equation and focusing equation in dispersion direction are respectively as follows:

$$d_0(\sin\alpha + \sin\beta) = m\lambda, \quad (2)$$

$$r = \frac{rR\cos^2\beta}{r[\cos\alpha + \cos\beta - 2b_2(\sin\alpha + \sin\beta)] - R\cos^2\alpha}, \quad (3)$$

式中  $d_0$  为光栅中心的刻线宽度, 也称为公称线宽,  $R$  为光栅基底的曲率半径,  $b_2$  为光栅线密度参数, 选择合适的值可以使光栅聚焦面近似为一平面。

Where  $d_0$  is the scale line width of grating center, also called nominal line width;  $R$  is the radius of curvature of grating substrate;  $b_2$  is the linear density parameter of grating. By selecting appropriate values, the focusing surface of the grating can be approximately a plane.

本文选取 Shimadzu 的 30-001 型光栅, 该光栅公称线密度  $n_0$  2 400 线/mm, 工作波长范围 1 ~ 6 nm, 入射臂长 237 mm, 入射角 88.65°。图 4 给

出了该光栅不同入射角对应的聚焦曲线, 坐标系定义与图 3 中一致, 光栅参数来自于文献 [19]。可以看出, 入射角 88.65° 时, 光栅中心到探测面距离  $D_0$  为 235 mm。不同入射角的聚焦曲线不同, 但是都可以拟合成直线, 因此可以根据需要改变光栅的使用结构参数。

Shimadzu 30-001 grating is selected. The parameters of the grating are the following: nominal linear density  $n_0$  is 2 400 lines/mm; wavelength range is 1 ~ 6 nm; incidence arm length is 237 mm, and incidence angle is 88.65°. Fig. 4 shows the focusing curves at different incidence angles, where the coordinate system definition is in line with that in

Fig. 3 , and grating parameters come from the reference [19]. As shown in Fig. 4 , when the incidence angle is  $88.65^\circ$  , the distance  $D_0$  from the grating center to the detection surface is 235 mm. Focusing curves at different incidence angles are different ,but all of them can be fitted into straight lines , so the structure parameters of the grating can be changed as needed.

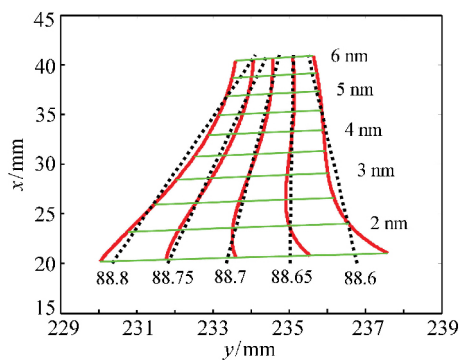


图 4 不同入射角对应的聚焦曲线, 红线表示聚焦曲线, 黑色虚线表示其拟合直线, 绿线表示不同波长

Fig. 4 Focusing curves and fitting straight lines at different incidence angles. The red lines represent the focus curves , the black dashed lines are straight fitting lines and the green lines are different wavelengths

### 2.3 装配方案优化

#### Assembly scheme optimization

光栅常规的装配方案是 CCD 平面与光栅中心的切平面垂直, 如图 5 ( a ) 所示, 这样的方案在实际使用中存在很大的困难, 一方面, 入射角的精度要求太高, 需要借助高精度的调整机构和测量装置反复调试来保证; 另一方面, CCD 与光栅联系紧密, 调整光栅姿态时, CCD 也必须相应调整, 提高了调整的难度。

The conventional grating assembly scheme is that the CCD plane is vertical to the tangent plane of the grating center , as shown in Fig. 5. Such scheme is very difficult in an actual application. On one hand , there are too high requirements for the incidence angle precision , and it can be guaranteed with

the aid of a high precision adjusting mechanism and measuring device. On the other hand , CCD is closely linked with the grating. When the grating attitude is adjusted , CCD must be adjusted accordingly , thereby increasing the adjustment difficulty.

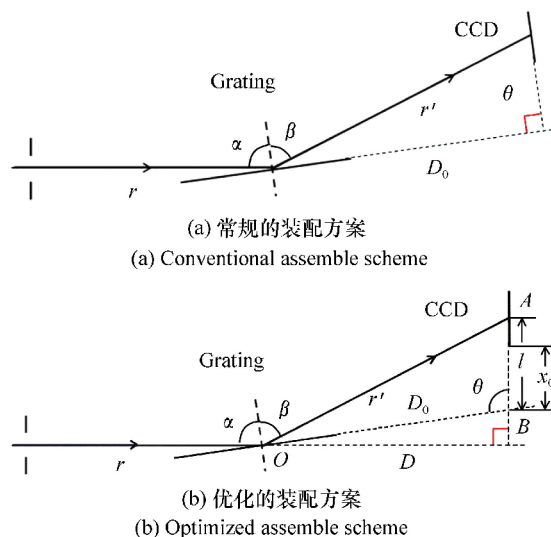


图 5 光栅的不同使用结构

Fig. 5 Structures of the grating ( a ) the conventional scheme , ( b ) the optimized scheme

为了可以分开独立调整光栅和 CCD ,我们以 CCD 平面与入射光线方向垂直作为目标对装配结构进行优化, 如图 5 ( b ) 所示, 这样得到的方案下, CCD 的倾角不再依赖光栅, 从而可以先安装调整好 CCD 再调节光栅, 在真空中只需要转动光栅, 使特定波长的谱线的像最窄, 就可以获得较高的安装精度。入射角  $\alpha$  取  $88.6^\circ$  进行设计, 利用公式 ( 2 ) 和公式 ( 3 ) , 以聚焦曲线的拟合直线与入射光线方向垂直为目标, 获得了对应的最佳入射臂长  $r$  和光栅中心到 CCD 探测面的距离  $D$  , 结果见表 1。这样在安装时就只有光栅需要在真空中调整, 同时也降低了入射角的调整难度。

In order that the grating and CCD can be adjusted separately , the assembly structure has been optimized by aiming at making the CCD plane be vertical to the incident ray direction , as shown in Fig. 5 ( b ) . In such scheme obtained , the dip angle of the CCD doesn't rely on the grating any longer , so that the CCD can be firstly installed and adjusted well

and then the grating is adjusted. High installation precision can be obtained by only turning the grating in vacuum to make the image of the spectral line of the specific wavelength be the narrowest. The incidence angle  $\alpha$  is taken as  $88.6^\circ$  in the design. Using formulas (2) and (3) and aiming at making the fitting straight line of the focusing curve vertical to the incident ray direction, the corresponding optimum incidence arm length  $r$  and distance  $D$  from the grating center to the CCD detection surface have been obtained. The result is shown in Tab. 1. Thus, only the grating needs to be adjusted in vacuum during installation, which also reduces the difficulty in incidence angle adjustment.

表 1 优化的装配方案参数

Tab. 1 Parameters of the optimized installation scheme

Parameters	$\alpha/(^\circ)$	$r/\text{mm}$	$D/\text{mm}$	$\theta/(^\circ)$
Value	88.6	270	234.0	91.4

### 3 分辨率 Resolution

分辨率是光谱类仪器的重要指标。本文设计的谱仪的分辨率主要受入射狭缝的宽度  $S_1$ 、光栅的衍射极限和像差、CCD 像元尺寸  $S_2$  等多项因素的影响,狭缝宽度和光栅性能决定了单色波长谱线的半高宽,像元尺寸则限制了谱仪的极限分辨率。

Resolution is an important index of an optical spectrum instrument. The resolution of the spectrometer designed in this paper is affected mainly by multiple factors such as entrance slit width  $S_1$ , grating's diffraction limit and aberration, CCD pixel size  $S_2$ , etc. Slit width and grating performance decide the FWHM of monochromatic wavelength spectral line, and pixel size limits the limiting resolution of the spectrometer.

由光栅方程结合几何关系可得,光栅在探测面上的线色散为:

According to the grating equation coupled with the geometrical relationship, the linear dispersion of the grating on the detection surface can be obtained as follows:

$$\frac{dl}{d\lambda} = \frac{mD}{d_0 \sin^2(\alpha + \beta - \pi/2) \cos\beta} \quad (4)$$

若已知某波长的光谱像的半高宽 FWHM,则可以得到该波长的线宽为:

If the FWHM of the spectral image at a wavelength is known, the line width of this wavelength can be obtained as follows:

$$\Delta\lambda = \frac{d \sin^2(\alpha + \beta - \pi/2) \cos\beta \cdot \text{FWHM}}{mD} \quad (5)$$

利用光线追迹<sup>[20]</sup>可以获取特定波长的谱线在探测面上的光谱像,从而综合分析入射狭缝宽度和光栅性能的影响。狭缝宽度设为  $100 \mu\text{m}$ ,入射臂长为  $270 \text{ mm}$ ,入射角为  $88.6^\circ$ ,光谱探测面放置在  $D = 234 \text{ mm}$  处,令光线在入射范围内随机生成,可以模拟获得探测面上的点列图。通过统计宽度方向上各个像素内的光线数量,得到光强统计分布图,对光强分布进行高斯拟合,求出半高宽,即可利用公式(5)计算线宽。图 6 为  $4.4 \text{ nm}$  波长的谱线光线追迹获得的点列图、统计直方图以及高斯拟合曲线,半高宽 FWHM 即像的宽度为  $13.8 \mu\text{m}$ ,对应线宽为  $0.0035 \text{ nm}$ 。图中横坐标表示谱线的像到入射光线的距离,对应于图 5(b) 中的长度  $l$ 。

The spectral image of the spectral line at a specific wavelength on the detection surface can be obtained using the ray tracing method<sup>[20]</sup>, thus comprehensively analyzing the influence of entrance slit and grating performance. The spot diagram on the detection surface can be obtained on the assumption that the slit width is  $100 \mu\text{m}$ , the incidence arm length is  $270 \text{ mm}$ , the incidence angle is  $88.6^\circ$ , the spectral detection surface is placed at  $D = 234 \text{ mm}$  and rays are generated randomly within the incidence range. The statistical distribution chart of

light intensity is obtained from the statistical analysis of rays of each pixel in the width direction. The FWHM is calculated through Gaussian fitting of the light intensity distribution, and then the line width can be calculated using formula (5). Fig. 6 shows the spot diagram, histogram and Gauss fitting curve

obtained using ray tracing at 4.4 nm. The FWHM i. e. image width is 13.8  $\mu\text{m}$ , and the corresponding line width is 0.0035 nm. In the figure, the abscissa denotes the distance from the spectral line image to the incident ray, which is corresponding with the length  $l$  in Fig. 5(b).

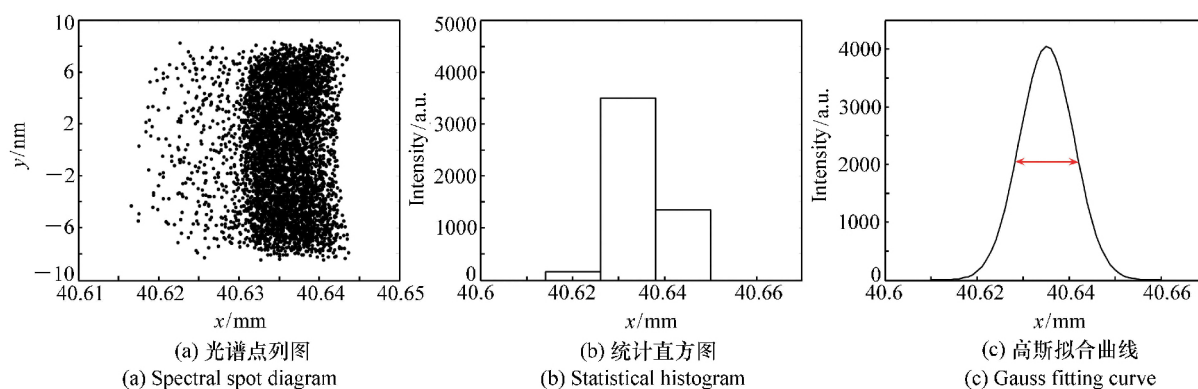


图6 4.4 nm 波长的光线追迹结果

Fig. 6 The result of ray tracing at 4.4 nm (a) Spot diagram, (b) Histogram, (c) Gauss fitting curve

受探测器像元尺寸的限制,光谱仪的分辨率往往不能直接由谱线线宽决定。根据奈奎斯特抽样定理,为了能真实反映信号特征,采样频率应大于信号频率的两倍,由公式(4)可以得到单个像元对应的谱线线宽  $\Delta\lambda_{s_2}$ ,则谱仪极限分辨率为  $Re_{\max} = \lambda/2\Delta\lambda_{s_2}$ 。像元宽度为 13  $\mu\text{m}$ , 4.4 nm 的半高宽小于像元尺寸的两倍,因此设计的谱仪可以实现极限分辨率 4.4 nm 处分辨率为 666,对应线宽 0.0066 nm。使用像元数 1 024 的 CCD,谱仪工作范围超过 3 nm,满足设计要求。

Limited by the pixel size of the detector, the resolution of the spectrometer cannot be determined directly by the spectral line width in general. According to Nyquist sampling theorem, the sampling frequency would be larger than twice of the signal frequency in order to truly reflect signal features. According to formula (4), the spectral line width corresponding with a single pixel can be obtained, and then the limiting resolution of the spectrometer is  $Re_{\max} = \lambda/2\Delta\lambda_{s_2}$ . The pixel width is 13  $\mu\text{m}$ , and the FWHM of 4.4 nm is less than twice of the pixel size, so the designed spectrometer can achieve the

limiting resolution, its resolution is 666 at 4.4 nm, and the corresponding line width is 0.0066 nm. The CCD with 1 024 pixels is used and the wavelength range of the spectrometer is over 3 nm, which meets the requirements of the design.

基于以上分析,本文设计的掠入射式近边 X 射线吸收谱仪的参数如表 2 所示。

表2 掠入射式近边 X 射线吸收谱仪设计参数  
Tab. 2 Design parameters of the Near-edge X-ray absorption spectrometer under grazing incidence conditions

Parameters	Value
Wavelength range/nm	2 ~ 5
Resolution	666@4.4 nm
$\varphi/(^\circ)$	2
Width of entrance slit $S_1/\mu\text{m}$	100
$n_0/\text{mm}^{-1}$	2 400
Incidence angle $\alpha/(^\circ)$	88.6
Incidence distance $r/\text{mm}$	270
$\theta/(^\circ)$	91.4
$D/\text{mm}$	234.0
Pixel size( $W \times H: \mu\text{m}^2$ )	13.5 $\times$ 13.5
Active pixels	1 024 $\times$ 1 024

According to the above analysis, the parameters of the near-edge X-ray absorption spectrometer under grazing incidence conditions designed in this paper are shown in Tab. 2.

#### 4 公差分析及装调方案设计

##### Tolerance analysis and assembly scheme design

根据前文的分析,为了使谱仪实现极限分辨率,谱线的半高宽应小于两个像元的尺寸,即

26  $\mu\text{m}$ , 而半高宽主要取决于入射狭缝、光栅和 CCD 之间的相对位置。图 7 给出了各参数的偏差对 4.4 nm 波长的半高宽的影响,可以看出,入射臂长  $r$  的误差  $\delta r$  对半高宽的影响几乎可以忽略, $D$ 、 $\theta$  和  $\alpha$  的偏差主要表现为向系统引入离焦像差,而半高宽对入射角  $\alpha$  的变化最为敏感。综合考虑各参数的作用,结合机械结构的调整能力,确定  $r$ 、 $D$ 、 $\theta$ 、 $\alpha$  的公差分别为  $\pm 1$  mm、 $\pm 0.1$  mm、 $\pm 0.5^\circ$ 、 $\pm 0.04^\circ$ ,谱线在极限误差下的半高宽为 24.8  $\mu\text{m}$ , 满足设计要求。

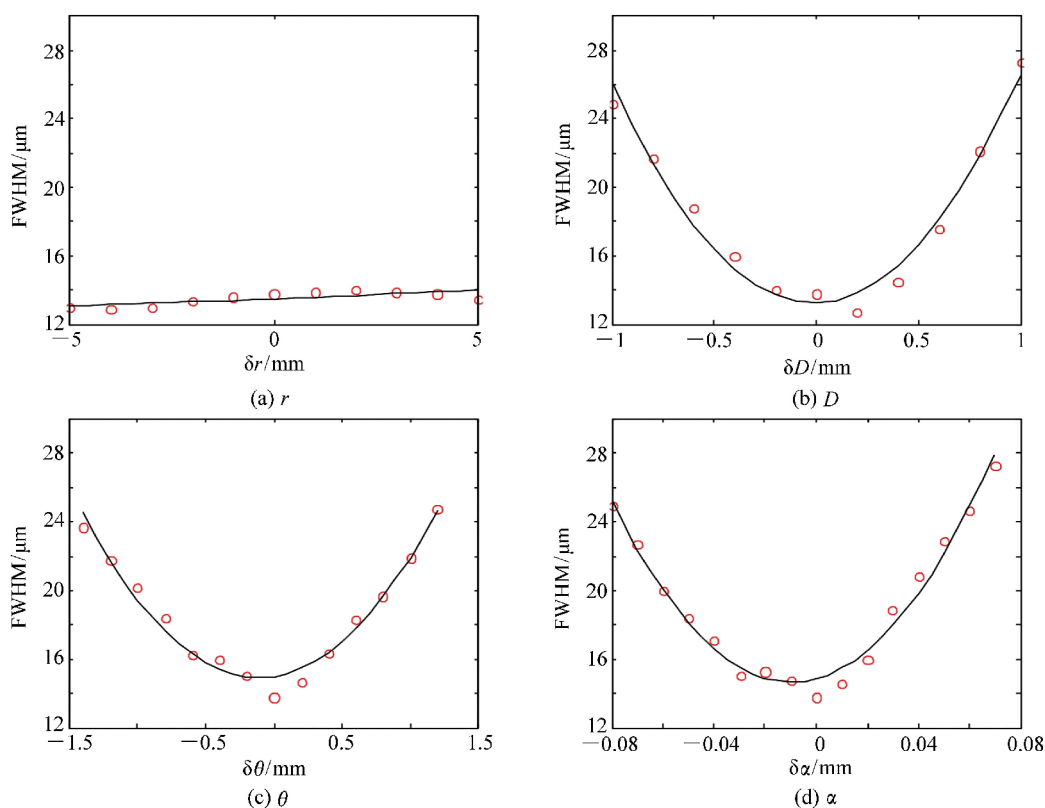


图 7 各参数( $r$ 、 $D$ 、 $\theta$ 、 $\alpha$ )的误差对 4.4 nm 单色谱线的半高宽的影响

Fig. 7 Influence of the error of each parameter on the FWHM at 4.4 nm (a)  $r$ , (b)  $D$ , (c)  $\theta$ , (d)  $\alpha$

According to the previous analysis, in order to achieve the limiting resolution of the spectrometer, the FWHM of spectra line would be less than the size of two pixels, *i. e.* 26  $\mu\text{m}$ . The FWHM depends mainly on the relative position among the entrance slit, grating and CCD. Fig. 7 shows the influence of the error of each parameter on the FWHM at 4.4 nm. As shown in the figure, the influence of

the error  $\delta r$  of the incidence arm length  $r$  on the FWHM can be neglected, the error of  $D$ ,  $\theta$  and  $\alpha$  is manifested mainly as the defocus aberration introduced to the system, and the FWHM is the most sensitive to the variation of the incidence angle  $\alpha$ . Comprehensively considering the role of each parameter in combination with the adjusting capacity of the mechanical structure, the tolerance of  $r$ ,  $D$ ,  $\theta$  and  $\alpha$

is determined to be  $\pm 1 \text{ mm}$ ,  $\pm 0.1 \text{ mm}$ ,  $\pm 0.5^\circ$  and  $\pm 0.04^\circ$  respectively, and the FWHM of spectral line at the limiting error is  $24.8 \text{ }\mu\text{m}$ , which meets the requirements of the design.

公差分析结果表明,在本文优化的方案下, $r$ 、 $D$ 和 $\theta$ 可以在大气环境中使用常规方法测量并调整到位,在真空环境中利用高精度电动转台连续改变 $\alpha$ ,使氮气等离子体发出的 $2.8787 \text{ nm}$ 谱线的半高宽最小,从而可以满足入射角的高精度要求。

According to the tolerance analysis result, using the optimized scheme in this paper,  $r$ ,  $D$  and  $\theta$  can be measured in atmospheric environment with a conventional method and well adjusted. In addition,  $\alpha$  is changed continuously in vacuum environment using a high precision electric rotary table so as to minimize the FWHM of the  $2.8787 \text{ nm}$  spectral line emitted by nitrogen plasma, which can thus meet the high precision requirements of incidence angle.

## 5 分辨率测试与波长标定

### Resolution test and wavelength calibration

图8展示了搭建完成的小型掠入射式近边X射线吸收谱仪。光谱仪工作在 $10^{-4} \text{ Pa}$ 真空环境下。沿着光路方向(在图中标注光源、各个腔体)3个真空腔体分别为光源室、样品室和光栅室,激光聚焦到喷出的气体团上形成等离子体,产生X射线辐射输出,经Ti膜后照射到样品表面,Ti膜用于过滤带外光。为了结构紧凑,入射狭缝安置在样品室中,CCD通过波纹管与光栅室相连,以便通过调整机构微调CCD位置。

Fig. 8 shows the well-erected compact near edge X-ray absorption spectrometer under grazing incidence conditions. The spectrometer works in  $10^{-4} \text{ Pa}$  vacuum environment. Along the light path direction (light source and each chamber marked in the figure), the three vacuum chambers are light source chamber, sample chamber and grating chamber re-

spectively. Laser is focused onto the ejected gas clumps to form plasma and generate X-ray radiation output. After passing through the Ti membrane, rays shine on the sample surface. The Ti membrane is used to filter out-of-band lights. In order to achieve a compact structure, the entrance slit is placed in the sample chamber, and the CCD is connected with the grating chamber via the corrugated pipe, for convenience of micro-adjusting the CCD position through the adjusting mechanism.

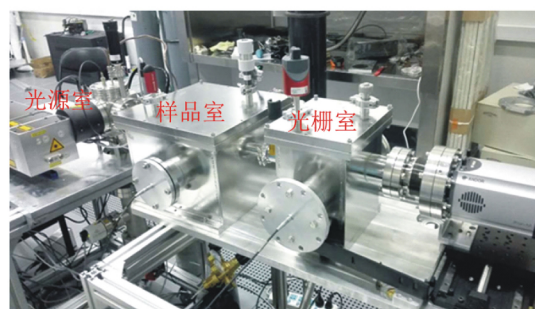


图8 光谱仪实物图

Fig. 8 Picture of the spectrometer

氮气作为激光等离子体光源靶材对光谱仪分辨率进行测试,图9为实验测得的光谱图。可以看出,氮气在 $2 \sim 5 \text{ nm}$ 波段的谱线均清晰可见,波长 $2.478 \text{ nm}$ 和 $2.49 \text{ nm}$ 两条谱线也能明显区分。对这两个光谱峰进行高斯拟合得到曲线C1和C2,曲线C1的半高宽FWHM为 $1.9$ ,不足两个像元,表明搭建的光谱仪可实现极限分辨,满足设计指标。

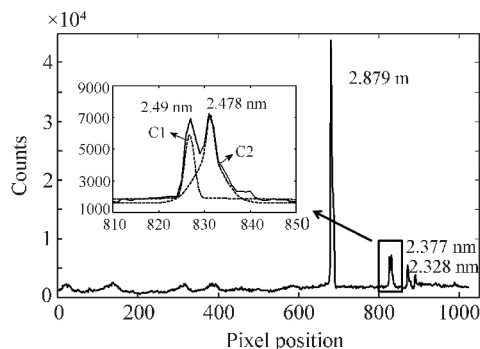


图9 氮气等离子体谱线

Fig. 9 Spectrum of  $\text{N}_2$  plasma

The resolution of the spectrometer has been tested using nitrogen as the laser plasma source target. Fig. 9 shows the spectrogram obtained from the test. It can be seen that the spectral lines of nitrogen at 2 – 5 nm are clearly visible and the two spectral lines at 2.478 nm and 2.49 nm can also be identified obviously. The curves C1 and C2 are obtained from Gauss fitting of the two spectral peaks. The

HWHM of curve C1 is 1.9 that is less than two pixels, indicating that the erected spectrometer can achieve the limiting resolution and the design index.

采用参数拟合法<sup>[19]</sup>进行波长标定,模型如式(6)所示:

Wavelength calibration is performed using the parameter fitting method<sup>[19]</sup>. The model is shown in formula (6).

$$\lambda = \frac{1}{m_0 \cdot n_0} \left( \sin\alpha - \frac{D_0 + [x_0 + (1024 - N) \cdot S_2] \cdot \sin\theta}{\sqrt{D_0^2 + 2\cos\theta \cdot D_0 \cdot [x_0 + (1024 - N) \cdot S_2] + (x_0 + N \cdot S_2)^2}} \right), \quad (6)$$

式中,各参数的定义参考图 5(b),  $N$  为 CCD 像素的位置,上边缘对应  $N$  为 0 的位置,  $n_0$  表示光栅的公称线密度。表 3 给出了像素位置对应的实际波长和标定波长,结果显示波长标定的误差小于 0.001 nm,光谱仪实际工作波长范围 2 ~ 5 nm。

CCD pixel, the upper edge is the position at  $N = 0$ , and  $n_0$  denotes the nominal linear density of the grating. Tab. 3 shows the actual wavelength and calibration wavelength at pixel positions. The results show that the wavelength calibration error is less than 0.001 nm and the actual wavelength range of the spectrometer is 2 – 5 nm.

Refer to Fig. 5(b) for the definition of each parameter in the above formula.  $N$  is the position of

表 3 波长标定结果

Tab. 3 Results of wavelength calibration

Pixel positions	1	631	777	782	821	841	1 024
Actual wavelength/nm		2.878 7	2.489 8	2.478 1	2.377 4	2.327 7	
Calibration wavelength/nm	5.025	2.878 1	2.490 2	2.477 5	2.378 2	2.328 1	2.008 3
Error/nm		-0.000 6	0.000 4	-0.000 5	0.000 8	0.000 4	

利用参数拟合法标定波长可以反求出系统各参数的实际值,并与理论设计值进行比较,结果如表 4 所示,可见各参数的实际值与设计值基本吻合,偏差均满足公差分配要求。

with the parameter fitting method. The actual value is compared with the theoretical design value. The result is shown in Tab. 4. As shown in the table, the actual value of each parameter is basically consistent with the design value, and all deviations meet the tolerance distribution requirements.

The actual value of each parameter of the system can be calculated through wavelength calibration

表 4 光学系统参数设计值与实际值比较

Tab. 4 Comparison of the design value with the actual value of optical system parameters

Parameters	$\alpha / (^\circ)$	$\theta / (^\circ)$	$D_0 / \text{mm}$	$x_0 / \text{mm}$
Design value	88.6	91.4	234	23.74
Actual value	88.634 8	91.389 9	234.011 3	23.682 6

## 6 结 论

### Conclusion

采用激光等离子体光源、球面变栅距光栅和面型 CCD 设计了一台用于研究有机物的碳 1s NEXAFS 谱掠入射式近边 X 射线吸收谱仪, 掠入射角取  $2^\circ$ 。为了方便调节光学元件的相对位置和姿态, 以探测面与入射光线垂直为目标对安装参数进行了优化, 得到了光栅入射角  $88.6^\circ$  时的安装方案, 入射臂长 270 mm, 光栅中心到 CCD 探测面垂直距离 234.0 mm。利用光线追迹的方法模拟了谱仪的光谱, 缝宽  $100\ \mu\text{m}$  时光谱仪在 4.4 nm 处的分辨率达到 666, 可以满足研究碳 1s NEXAFS 谱的要求。分析了各装配参数的误差对 4.4 nm 处分辨率的影响, 确定了  $r$ 、 $D$ 、 $\theta$ 、 $\alpha$  的公差分别为  $\pm 1\ \text{mm}$ 、 $\pm 0.1\ \text{mm}$ 、 $\pm 0.5^\circ$ 、 $\pm 0.04^\circ$ , 据此设计了谱仪的装调方案。最后通过测量氮气等离子体光谱, 对光谱仪性能进行了测试, 结果显示, 谱仪各项性能满足设计要求。

In order to study the NEXAFS spectrum of the organic material carbon(1s), we design a near edge X-ray absorption spectrometer under grazing incidence conditions using a laser-produced plasma source, an aberration corrected flat-field grating and a planar CCD. The grazing incidence angle of the

spectrometer is taken as  $2^\circ$ . In order to conveniently adjust the relative position and attitude of optical elements, the installation parameters have been optimized aiming at making the detection surface vertical to the incident ray direction. The optimized installation scheme where the incidence angle of the grating is  $88.6^\circ$  has been obtained. The incidence arm length is 270 mm, and the vertical distance from the grating center to the CCD detection surface is 234.0 mm. Using the ray tracing method, the spectrum of the spectrometer has been simulated. When the slit width is  $100\ \mu\text{m}$ , the resolution of the spectrometer reaches 666 at 4.4 nm, which can meet the requirements of research on the NEXAFS spectrum of carbon(1s). The influence of the error of each assembly parameter on the resolution at 4.4 nm has been analyzed, and the tolerance of  $r$ ,  $D$ ,  $\theta$  and  $\alpha$  has been determined to be  $\pm 1\ \text{mm}$ ,  $\pm 0.1\ \text{mm}$ ,  $\pm 0.5^\circ$  and  $\pm 0.04^\circ$ , respectively. Based on above parameters, the assembly scheme of the spectrometer has been designed. Finally the performance of the spectrometer has been tested by measuring nitrogen plasma spectrum. The results show that all performance indexes of the spectrometer meet the design requirements.

### 参考文献:

- [1] 马礼敦. X 射线吸收光谱及发展[J]. 上海计量测试 2007 34(6): 2-11.  
MA L D. X-ray absorption Spectroscopy and its developments[J]. *Shanghai Measurement & Testing* 2007 34(6): 2-11. (in Chinese)
- [2] GROOT D. XANES spectra of transition metal compounds[J]. *Journal of Physics: Conference Series* 2009 190(1): 111-116.
- [3] WEISS K, WOELL C, JOHANNSAMANN D. Near-surface molecular orientation in polymeric alignment layers: a NEXAFS investigation[J]. *Proceedings of SPIE* 1999 3800: 104-111.
- [4] 潘宵. 聚合物光电器件中金属/聚合物界面结构与性质的研究[D]. 合肥: 中国科学技术大学 2015.  
PAN X. The structures and properties of metal/polymer interfaces in polymer-based photoelectronic devices[D]. Hefei: University of Science and Technology of China 2015. (in Chinese)
- [5] 李辉, 高强, 王帅 等. 同步辐射软 X 射线近边吸收谱方法研究长期施肥对黑土有机氮官能团的影响[J]. 光谱学与光谱分析 2015(7): 2038-2042.  
LI H, GAO Q, WANG SH *et al.*. Effect of long-term fertilization on organic nitrogen functional groups on black soil as revealed by synchrotron-based X-ray absorption near-edge structure spectroscopy[J]. *Spectroscopy and Spectral Analysis*, 2015(7): 2038-2042. (in Chinese)
- [6] BRAUN A. Carbon speciation in airborne particulate matter with C(1s) NEXAFS spectroscopy[J]. *Journal of Environ-*

- mental Monitoring Jem* 2005 7( 11) : 1059-65.
- [7] NOV KOV E ,MITREA G ,PETH C *et al.* . Solid supported multicomponent lipid membranes studied by x-ray spectromicroscopy [J]. *Biointerphases* 2008 3( 2) : FB44-FB54.
- [8] YODA O ,MIYASHITA A ,MURAKAMI K *et al.* . Time-resolved X-ray absorption spectroscopy apparatus using laser plasma as an X-ray source [J]. *Proceedings of SPIE* ,1991 ,1503: 463-466.
- [9] NAKANO H ,GOTO Y ,LU P *et al.* . Time-resolved soft X-ray absorption spectroscopy of silicon using femtosecond laser plasma X-rays [J]. *Applied Physics Letters* ,1999 ,75( 16) : 2350-2352.
- [10] BECK M ,VOGT U ,WILL I *et al.* . A pulse-train laser driven XUV source for picosecond pump probe experiments in the water window [J]. *Optics Communications* 2001 ,190( 1-6) : 317-326.
- [11] VOGT U ,WILHEIN T ,STIEL H *et al.* . High resolution X-ray absorption spectroscopy using a laser plasma radiation source [J]. *Review of Scientific Instruments* 2004 ,75( 11) : 4606-4609.
- [12] PETH C ,BARKUSKY F ,SEDLMAIR J *et al.* . Near-edge X-ray absorption fine structure measurements using a laser plasma XUV source [J]. *Journal of Physics: Conference Series* 2009 ,186( 1) : 012032.
- [13] SEDLMAIR J ,GEBER S ,PETH C *et al.* . NEXAFS spectroscopy with a laser plasma X-ray source on soil samples [J]. *Journal of Physics: Conference Series* 2009 ,186( 1) : 012034.
- [14] 薛守庆 薛兆民. 二次掺杂聚吡咯/聚噻吩膜的制备及其光电性能 [J]. 发光学报 2016 37( 9) : 1124-1129.  
XUE SH Q ,XUE Z M. Preparation and anti-corrosive performance of Ppy/PTh composites redoped with zinc phosphate [J]. *Chinese Journal of Luminescence* 2016 37( 9) : 1124-1129.
- [15] 邹凤君 范思大 谢强 等. 掺杂石墨烯量子点对 P3HT: PCBM 太阳能电池性能的影响 [J]. 发光学报 2016 37( 9) : 1082-1089.  
ZOU F J ,FAN S D ,XIE Q *et al.* . Effect of doping graphene quantum dots on the performance of P3HT: PCBM Solar Cells [J]. *Chinese Journal of Luminescence* 2016 37( 9) : 1082-1089.
- [16] 彭博 曹亚鹏 胡煜峰 等. P3HT/PMMA 双层聚合物电双稳器件的研究 [J]. 发光学报 2016 37( 9) : 1090-1096.  
PENG B ,CAO Y P ,HU Y F *et al.* . Polymer bistable devices based on poly( 3-hexylthiophene) / poly( methylmethacrylate) bilayer films [J]. *Chinese Journal of Luminescence* 2016 37( 9) : 1090-1096.
- [17] ANDERSON C. Center for X-Ray Optics: <http://www-cxro.lbl.gov/>.
- [18] HARADA T ,KITA T. Mechanically ruled aberration-corrected concave gratings [J]. *Applied Optics* ,1980 ,19( 23) : 3987-3993.
- [19] 杜学维. 凹面变线距光栅的二维线密度分布测试及软 X 射线平场光谱仪的研制 [D]. 合肥: 中国科学技术大学 , 2013.  
DU X W. Measurement of groove density 2D distribution of concave VLS grating and construction of a soft X-ray flat field spectrograph [D]. Hefei: University of Science and Technology of China 2013. ( in Chinese)
- [20] LAI B ,CERRINA F. SHADOW: a synchrotron radiation ray tracing program [J]. *Nuclear Instruments & Methods in Physics Research* ,1986 246( 1-3) : 337-341.

## 作者简介:



陈晨曦阳( 1991—) ,男,江苏南通人,硕士研究生,主要从事 X 射线吸收谱仪方面的研究。E-mail: chenchenxiyang@163.com  
CHEN Chen-xi-yang ( 1991—) : male , born in Nantong , Jiangsu; master degree candidate; engaged mainly in the study of X - ray absorption spectrometers. E-mail: chenchenxiyang@163.com



金春水( 1964—) ,男,吉林长春人,博士,研究员,博士生导师,主要从事紫外极紫外光学技术方面的研究。E-mail: Jincs@sklao.ac.cn  
JIN Chun-shui ( 1964—) , male , born in Changchun , Jilin; doctor , researcher; engaged mainly in the study of UV and EUV optical technologies. E-mail: Jincs @ sklao. ac. cn